ELSEVIER

Materials Science and Engineering A357 (2003) 376–385

MATERIALS SCIENCE & ENGINEERING A

www.elsevier.com/locate/msea

Effect of SiC particle dispersion on microstructure and mechanical properties of polymer-derived SiC/SiC composite

Masaki Kotani [a,*], Takahiro Inoue [b], Akira Kohyama [c], Yutai Katoh [c], Kiyohito Okamura [d]

[a] *Graduate School of Energy Science, Kyoto University, Yoshida-Honmachi, Sakyo-ku, Kyoto 606-8501, Japan*
[b] *National Institute of Advanced Industrial Science and Technology, 1-2-1 Namiki, Tsukuba, Ibaraki 305-8942, Japan*
[c] *Institute of Advanced Energy, Kyoto University, Gokasho, Uji, Kyoto 611-0011, Japan*
[d] *Graduate School of Engineering, Osaka Prefecture University, 1-1 Gakuen-cho, Sakai, Osaka 599-8531, Japan*

Received 5 February 2003

Abstract

To improve the performance of SiC fiber-reinforced SiC matrix composite (SiC/SiC composite), a polymer impregnation and pyrolysis process (PIP process) has been developed by incorporating an inert filler with polyvinylsilane. Composites consolidated with slurries of various filler contents were thoroughly examined at each repetition of the PIP process. The fiber volume fraction and matrix microstructure in the composites were determined during consolidation as a function of the filler content. Densification behavior during multiple PIP processing was much dependent on the microstructure formed in consolidation. Transmission electron microscopy revealed the effect of filler content on the microstructure of the matrix and of the fiber/matrix interface. In addition, the relationships between the microstructure and the mechanical properties were evaluated from a fundamental viewpoint.

Keywords: SiC fiber-reinforced SiC matrix composite; PIP process; Filler content; Fiber volume fraction; Polymer-derived microstructure

1. Introduction

Since silicon carbide has superior characteristics as a structural material from the viewpoints of its thermal and mechanical properties, chemical stability and low radioactivation, there have been many efforts to develop SiC fiber-reinforced SiC matrix composites (SiC/SiC composites) for use in aerospace and advanced energy systems [1–3]. As a promising candidate for the fabrication of SiC/SiC composites, the polymer impregnation and pyrolysis process (PIP process), which comprises the impregnation of a polymeric precursor into a fibrous preform, together with pyrolysis, has been widely applied [4–11]. The organosilicon polymer route to produce SiC-based ceramic composites is advantageous in the following aspects: (1) high impregnation efficiency into the fiber-preform via the liquid phase; (2) controllability of microstructure, nanostructure and chemical composition; and (3) the technical applicability of fiber-reinforced plastics or carbon fiber-reinforced carbon matrix composites (C/C composites) [12–14]. However, sufficient densification in bulk component production is very difficult due to significant volume shrinkage and gas evolution of a polymer precursor during pyrolysis [15–17], which has led this technique to be applied industrially only to the preparation of low-dimensional components such as ceramic coatings [18], powders and fibers [19–21] for many years. Even though recent studies of SiC precursors have proved the feasibility of high-strength monolithic SiC production by intermediate powder routes [22,23], it still remains difficult for polymeric methods to be applied to the fabrication of dense SiC/SiC composites because of the requirements for impregnation. Because the mechanical properties of ceramic matrix composites were well

* Corresponding author. Address: Thermal Engineering Group, Office of Research and Development, National Space Development Agency of Japan, Tsukuba Space Center 2-1-1 Sengen, Tsukuba, Ibaraki 305-8505, Japan. Tel.: +81-298-68-2336; fax: +81-298-68-2968.
E-mail address: kotani.masaki@nasda.go.jp (M. Kotani).

0921-5093/03/$ - see front matter
doi:10.1016/S0921-5093(03)00206-5

Table 1
Densities of the constituents

Constituent	Density (Mg m^{-3})
Hi-Nicalon™	2.74
Betarundum™ (Ultrafine)	3.20
PVS (R.T.)	0.91
Pyrolyzed product of PVS (1473 K)	2.68
PCS (R.T.)	1.12
Pyrolyzed product of PCS (1473 K)	2.70

known to depend on matrix microstructure, i.e. porosity, pore size and crystallinity, as well as fiber volume fraction and fiber/matrix interfacial properties, the development of a process to make homogeneous matrices with low porosity has been considered to be highly desirable. As the key issues, the volumetric yield of matrix precursor and the consolidation technique for making the ceramic body are important. In order to increase the volumetric yield of the precursor, filler loading of the polymer has been widely pursued [24,25]. To make a strong matrix with low porosity, a green body composed of fiber and matrix precursor needs to be well consolidated. To establish a process for high performance composite production, it is very important to clarify the effect of filler loading on the microstructure during consolidation.

In the present work, development of the PIP process was performed by systematically investigating the effect of filler content on the microstructure. In the consolidation processing, the effect of filler content on both porosity and the distribution of pores was mainly examined. In the multiple PIP processing, the densification behavior, which was designed to reduce porosity, was precisely monitored. In addition, a comparison of the densification efficiencies for polyvinylsilane (PVS) and polycarbosilane (PCS) [26–28] was carried out. Transmission electron microscopy (TEM) observation revealed the effects of filler content on the nanostructure of the matrix and fiber/matrix interface, and differences in the pyrolyzed matrix resulting from the use of PVS and PCS were clarified. The relationships between microstructure and mechanical properties are discussed as well.

2. Experimental

The polymeric precursors employed for the matrix were PVS and PCS. PVS is a transparent liquid with adequate stability in ambient air. It was developed by Mitsui Chemicals, Inc. (Japan) [29–32]. PCS has been widely used as a SiC precursor. It is a solid at room temperature. It was obtained from Nippon Carbon Co., Ltd (Japan). According to thermogravimetric analysis, the mass yields for PVS and PCS, obtained after pyrolysis up to 1473 K in Ar, were 32 and 68%, respectively. As the filler material for the matrix, beta-SiC particles with an average particle size of 0.27 μm were utilized. These are sold commercially as an ultrafine grade of Betarundum™ by the Ibiden Co., Ltd (Japan). Hi-Nicalon™ [33,34] was used as the reinforcement. This is a PCS-derived Si–C (–C) fiber produced by the Nippon Carbon Co., Ltd. Densities of each constituent are summarized in Table 1. For fibers and powders, values specified by the manufacturers were utilized. The values for the original polymers and for the products obtained after pyrolysis up to 1473 K in Ar were determined by picnometry. According to the changes of mass and density resulting from pyrolysis, the volumetric yields of PVS and PCS were estimated to be 11 and 28%, respectively.

Unidirectional composites were fabricated by the hand lay-up method. The process conditions were designed on the basis of the pyrolytic chemistry of the polymer precursors. Fiber preforms were prepared by hand filament-winding. Fiber tow was wound on a reel of 40×20 mm^2 at a nominal rate of 1 tow mm^{-1}. Desizing treatment of the fibers was performed at 873 K for 30 min in vacuum. No coating was applied on the fibers. The PVS-slurries were prepared in the ambient atmosphere. To make a prepreg sheet, the fibrous preform was compounded with the slurry in air. To cure the sheet, it was heated at a rate of 300 K h^{-1} in Ar. To make a green body, cured sheets were cut into plies of 40×20 mm^2 and stacked. This was then placed in a carbon mold for consolidation. The green body was consolidated at 300 K h^{-1} up to 1473 K in Ar under uniaxial pressure [35]. The thicknesses of the consolidated bodies varied depending on the filler content. For further densification, the consolidated body was subjected to six repetitions of subsequent PIP processing with PVS or PCS. These were performed under the same heating conditions as those for the consolidation performed under no applied pressure. For all operations, no solvent was added to the PVS, whereas hexane was added to PCS. No particles were loaded in this step.

Densitometry were performed by the Archimedean method after every repetition of PIP processing. This was usually done only once for one particular condition. Bulk density (d_{bulk}), apparent density (d_{apparent}) and open porosity (υ_{op}) could be obtained in this experiment. The bulk density was defined as the specific gravity of a rectangular sample. The apparent density was defined as the average density of all constituents involving closed pores. Open porosity was taken to be the volume fraction of open pores in the rectangular sample.

The procedure used for the densitometry was as follows. All open pores of the sample were filled with pure water by boiling for 2 h. The weight of the sample (W_{a}) was measured in pure water at room temperature. The water temperature (T) was also measured in order

to calculate its density ($\rho_{water(T)}$) accurately. Next, the sample was removed from the water, and surface water was quickly wiped off. The weight of the sample involving water in all open pores (W_b) was measured in the ambient atmosphere. Next, the sample was dried at 383 K for 2 h. The weight of the sample (W_c) was measured in the ambient atmosphere. Thus, d_{bulk}, $d_{apparent}$ and υ_{op} were obtained from the following equations.

$$d_{bulk} = \frac{W_c}{W_b - W_a}\rho_{water(T)} \quad (1)$$

$$d_{apparent} = \frac{W_c}{W_c - W_a}\rho_{water(T)} \quad (2)$$

$$\upsilon_{op} = \frac{d_{apparent} - d_{bulk}}{d_{apparent}} \times 100 \quad (3)$$

Also, the closed porosity (υ_{cp}) was calculated according to the following three equations:

$$\upsilon_f + \upsilon_{particle} + \upsilon_{pyro(n)} + \upsilon_{op(n)} + \upsilon_{cp(n)} = 100 \quad (4)$$

$$d_{bulk(n)} = \frac{\rho_f\upsilon_f + \rho_{particle}\upsilon_{particle} + \rho_{pyro}\upsilon_{pyro(n)}}{100} \quad (5)$$

$$\upsilon_{pyro(n)} = \upsilon_{pyro(0)} + \sum_{x=1}^{n} \frac{\rho_{pyro}(W_{bulk(x)} - W_{bulk(x-1)})}{V_{bulk(x)}} \times 100 \quad (6)$$

where ρ and υ are the density and volume fraction of each constituent, respectively. W_{bulk} is the dry weight of the composite; it corresponds to W_c. V_{bulk} is the volume of the composite, obtained from W_{bulk} multiplied by d_{bulk}. The subscripts f, pyro, op and cp represent fiber, polymer-pyrolyzed product, open-pore and closed-pore, respectively. The index n indicates the number of repetitions of subsequent PIP processing. Thus, the case of $n = 0$ corresponds to the consolidation step. Because the consolidation of the green body was accompanied by gas emission from the polymer, the calculation was performed under the assumption that there were no closed pores formed during consolidation ($\upsilon_{cp(0)} = 0$). The relative density, which was defined as the volume fraction of all constituents in the rectangular sample, was calculated as $100 - \upsilon_{op} - \upsilon_{cp}$ (%). The volume fraction of fiber (υ_f) was obtained by means of image analysis of scanning electron microscopy (SEM) micrographs. The porosity of the matrix (p_{matrix}) was calculated according to the following equation:

$$p_{matrix} = \frac{\upsilon_{op} + \upsilon_{cp}}{\upsilon_f} \times 100 \quad (7)$$

Metallographic analysis was performed for consolidated bodies and final composites with SEM. Further microstructural analysis of matrix and fiber/matrix interface was performed using a TEM with an acceleration voltage of 200 kV. Thin foils for TEM observation were prepared by the focused ion beam machining technique [36].

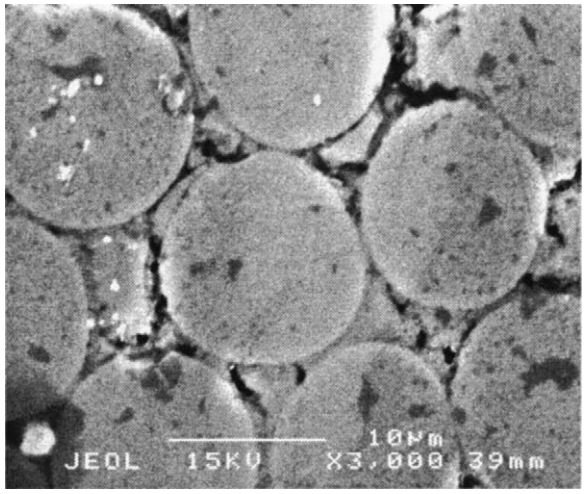

Fig. 1. SEM micrograph of a composite after seven repetitions of multiple PIP processing. No filler was loaded into the matrix precursor.

The mechanical properties of the composites were measured by use of a three-point flexural test with a span length of 25 mm and a crosshead speed of 0.5 mm min^{-1} at room temperature. The load was applied perpendicular to the fiber orientation. At least three specimens were measured for each condition. The nominal specimen dimensions were 30 mm (length) × 4 mm (width) × 1 mm (thickness). The actual dimensions were obtained by taking the average of several measured values with a micrometer. The ultimate flexural strength (σ_{uf}) was obtained from the maximum stress point. The work-of-fracture (WOF) was obtained from the integral of the load-crosshead displacement chart. To evaluate the stiffness of the composites comparatively, the tangent modulus of elasticity (E_f) was calculated from the steepest initial straight-line portion of the load-deflection curve [37].

3. Results and discussion

As the first stage of this work, a trial fabrication of PVS-derived composite was performed with no particulate loading. Fig. 1 represents a typical cross-sectional micrograph of the composite. PVS appeared to be impregnated well even into small area such as intra-bundle and showed good wettability with the Hi-Nicalon™ fibers. However, many cracks still remained over the entire matrix even after seven repetitions of subsequent PIP processing. Considering the great changes of mass and density during pyrolysis [26], these cracks should be formed due to volume shrinkage of the polymer. In order to reduce such flaws, the volumetric

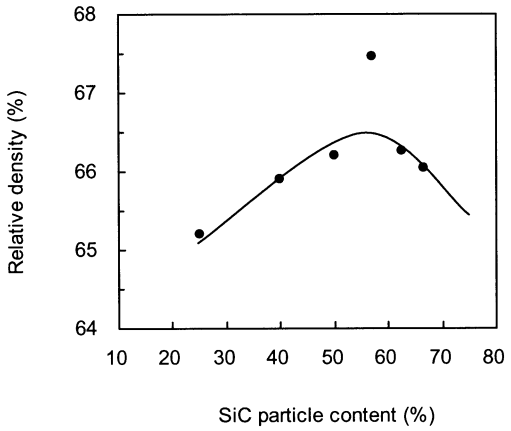

Fig. 2. Relative densities of the consolidated bodies as a function of SiC particle content.

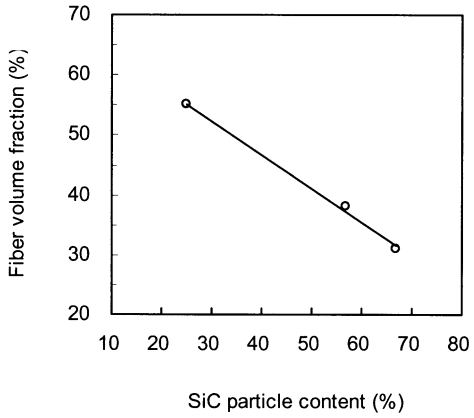

Fig. 4. Fiber volume fractions of the consolidated bodies, which were obtained by image analysis of SEM micrographs.

yield of matrix precursor needs to be improved. Particulate loading of the matrix precursor was considered to be a promising approach to achieve sufficient densification.

The work carried out on composite fabrication with SiC particle loading is described hereafter. Fig. 2 shows the relative densities of the consolidated bodies for various SiC particle contents. These increased as the filler content was raised to 57% and then decreased. The maximum value was obtained at a filler content of 57%, although the volumetric yield of the slurry improved continuously with increasing filler content. This feature suggested that high filler loadings might have a negative influence, impeding further densification. Therefore, it was considered that the effect of the filler loading on the microstructure of the consolidated body needs to be clarified in order to optimize the consolidation conditions.

Fig. 3 shows SEM micrographs of as-consolidated bodies prepared from slurries with SiC particle contents of (a) 25%, (b) 57%, and (c) 67%. From the low magnification micrographs (upper column), large pores can be identified in (a) and (b) but are very scarce in (c). From the high magnification micrographs (lower column), many micropores can be seen between the fibers in (a), a few in (b) and almost none in (c). The polymeric slurry could be well impregnated even at the high filler content of 67%. These microstructural features are quite consistent with the volumetric yield of the slurry, but are not consistent with the densitometry results, where the highest density was found at 57% filler content. The reason for this discrepancy will be explained below. Another important aspect of this figure is the fiber distribution. Uniform fiber distribution was seen for all composites. It was considered that this was accomplished by effective consolidation with SiC particles of

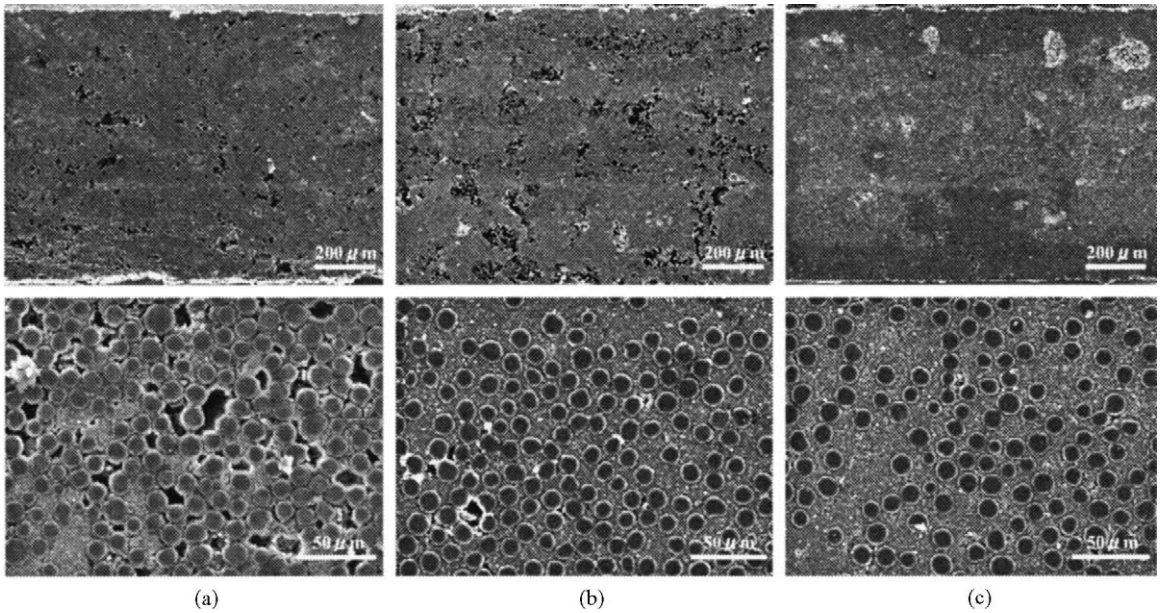

Fig. 3. SEM micrographs of the consolidated bodies with SiC particle content slurries of (a) 25%; (b) 57% and (c) 67%.

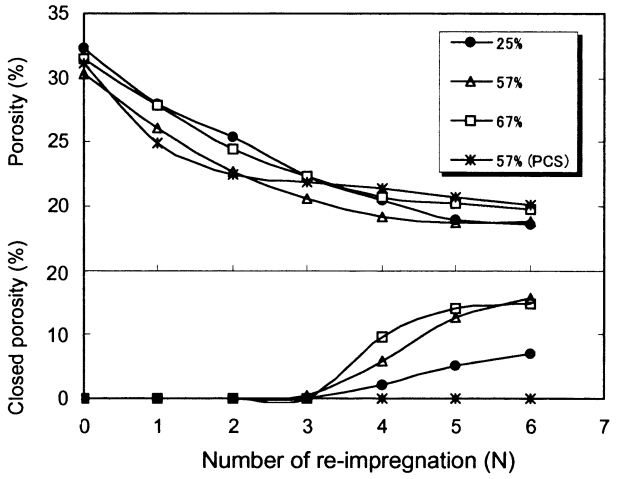

Fig. 5. Total and closed porosities of the composites as a function of the number of repetitions of subsequent PIP processing.

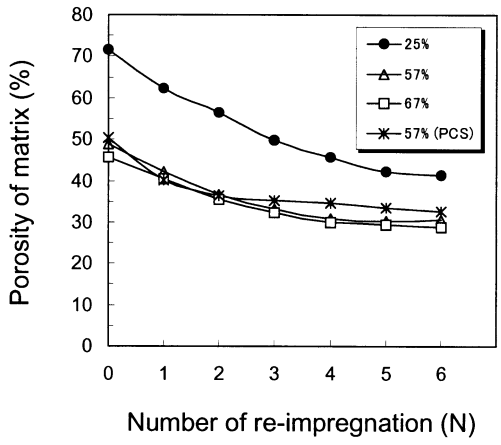

Fig. 6. Total porosities of matrices of the composites as a function of the number of repetitions of subsequent PIP processing.

suitable size under the conditions applied in the present work.

Fig. 4 represents the fiber volume fractions V_f of the consolidated bodies as a function of SiC particle content in the original slurry. This decreased continuously as the particulate loading was increased, even though the total volume of pyrolyzed product of the impregnated slurry was the same for all composites. This feature can be attributed to a decrease in the fluidity of the slurry with increasing particulate loading. In cases where the slurry retains sufficient fluidity, the slurry can be partly removed from the fiber preform under pressure, and thus the fibers can come into close contact with each other. Because V_f, as well as porosity, is well known to be one of the main factors in determining the mechanical properties of ceramics composites [38–40], consolidation techniques to maximize V_f are important, even if slurries of high filler content are utilized.

Fig. 5 shows the total porosity and closed porosity of the composites during multiple PIP processing. Continuous reductions in total porosity were observed for all filler contents. In particular, quite similar behavior was exhibited by all composites up to four repetitions of subsequent PIP processing. This stage is considered to be mainly attributable to the filling of large pores. The efficiency of porosity reduction declined gradually with increasing number of repetitions of PIP processing, and thus the composites with filler contents of 57 and 67% showed only a small change of porosity after four repetitions. In contrast, a further reduction of porosity was seen only for 25% filler, which resulted in the lowest porosity. This feature can be attributed to the filling of inter-fiber pores, many of which can be observed in Fig. 3. Changes in the closed porosity provide useful information with which to understand the densification behavior. This began to rise after the fourth repetition of subsequent PIP processing for all composites. It increased more rapidly when the filler content increased. The closed porosity for 67% filler content appeared to approach a limiting value after five repetitions of subsequent PIP processing, whereas those for 25 and 57% filler continued to increase further. Because a given composite is densified by the filling of preexisting pores with impregnated polymer-pyrolyzed product, closed pores would be formed due to insufficient permeation of the precursor or clogging of the pores with pyrolyzed product. The numbers of open pores distributed in the consolidated body decreased gradually as the processing proceeded, but some remained as closed pores. With respect to the permeability of the precursor, closed pores would be generated more easily as the sizes of the pores decreased. Therefore, the reason why closed porosity increased more rapidly as the filler content rose can be explained by the distribution of small pores. This expectation will be assessed below.

The densification efficiency of PVS was also compared with that of PCS in this figure (Fig. 5). The main differences between PVS and PCS as a matrix precursor were the ceramic yield and the state at room temperature. Because the densification behavior by multiple PIP processing was basically determined by the impregnation efficiency and the volumetric yield of a precursor, the effects of these two differences need to be examined closely. Concerning the ceramic yield, PCS (68%) was superior to PVS (32%). However, PCS always needed to be diluted with solvent as it remains in the solid state at room temperature. Dilution with solvent might reduce the quantity of precursor impregnated. According to the results in Fig. 5, PCS reduced the porosity more efficiently than PVS for the first two process repetitions. This might be due to the higher ceramic yield of PCS. However, after the third process repetition, only a slight reduction of porosity was observed for PCS, whereas the porosity decreased continuously for PVS. As another noticeable feature, almost no closed pores were formed

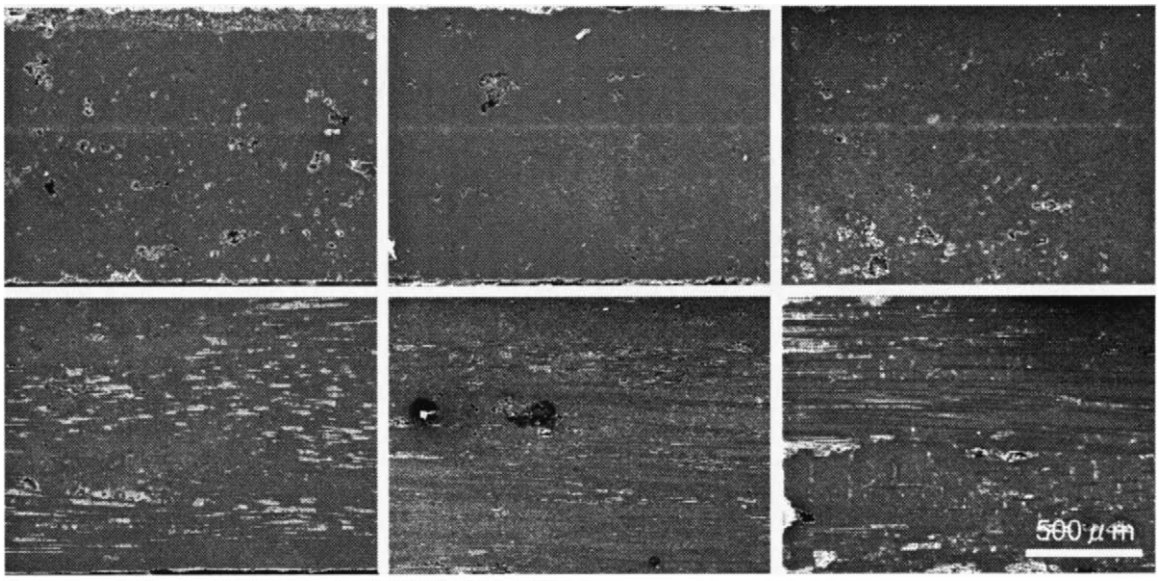

Fig. 7. SEM micrographs of the composites consolidated with various SiC particle content slurries (a) 25%; (b) 57%; (c) 67%, after six repetitions of subsequent PIP processing.

with PCS, which might be due to insufficient permeability of the PCS solution into small pores. It can be asserted that the permeability of PVS into very small pores was superior to that of the PCS solution under the present conditions. Therefore, it can be concluded that the ceramic yield of polymeric precursor is very important in the early stages of multiple PIP processing, and the physical characteristics such as permeability and wettability became influential as the porosity decreased further. In this work, PVS achieved densification superior to that for PCS after six repetitions of PIP processing, owing to its excellent permeability.

Porosities of the matrix were compared among the composites mentioned above, as shown in Fig. 6. In contrast to the porosities of the composites, quite simple features were found. The porosity after consolidation was dependent on the filler content. It decreased greatly going from 25 to 57% filler, while a small difference was seen going from 57 to 67% filler. This feature is closely related to the amounts of inter-fiber pores, as represented in Fig. 3. As for the change of porosity during multiple PIP processing, almost the same type of behavior was shown among the composites multiply densified with PVS. With increasing filler content, the porosity of the matrix, and also the fiber volume fraction, decreased. As the fiber used is a well-densified polymer-derived product [34], the reduction of fiber content leads to an increase in porosity of the composite. Therefore, the results of relative density shown in Fig. 2 were explained by the porosity of the matrix and the fiber volume fraction of the consolidated bodies. It will be mentioned in conjunction with the microstructural characteristics below.

Fig. 7 shows typical cross-sectional (upper column) and longitudinal (lower column) microstructures of the composites after six repetitions of subsequent PIP processing with PVS. Comparing these micrographs with those obtained after consolidation (Fig. 3), the numbers of pores, seen as white areas, decreased fairly significantly, but they still remained, depending on the filler content. Bulk densities of these composites were (a) 2.24 Mg m^{-3}, (b) 2.30 Mg m^{-3} and (c) 2.25 Mg m^{-3}, respectively. As a clear characteristic of the microstructure, a large number of small pores were distributed along the fiber direction in Fig. 7(a). These could not be filled due to drastic volumetric shrinkage of the precursor. On the other hand, some cracks were propagated perpendicular to the fiber direction in Fig. 7(c). These

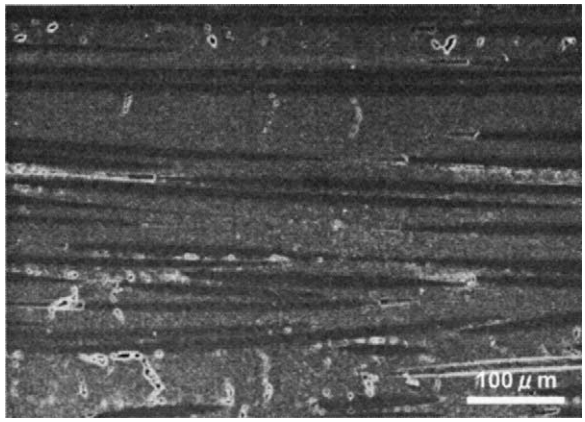

Fig. 8. SEM micrographs of the composites consolidated with a slurry of 67% filler content, showing the distribution of cracks initiated perpendicular to the fiber direction.

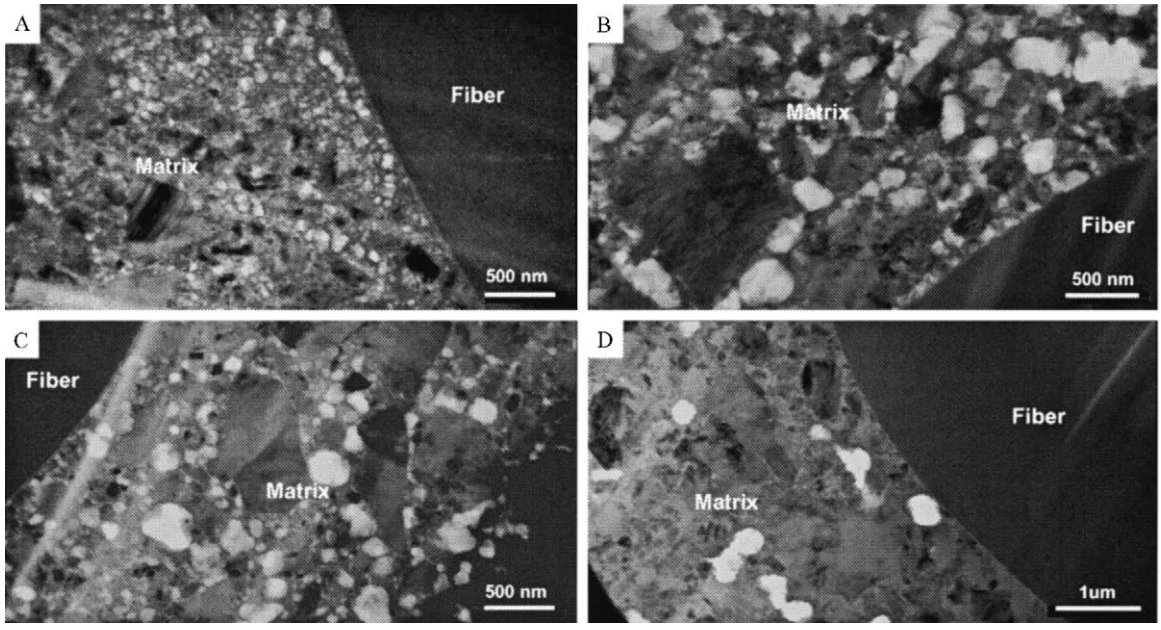

Fig. 9. TEM micrographs of composites consolidated with slurries of various SiC particle contents and multiply densified using PVS or PCS: (A) 25% PVS; (B) 57% PVS; (C) 67% PVS; (D) 57% PCS.

were initiated along the pressurization direction. As possible reasons for the crack generation, thermal mismatch between fiber and matrix, as well as pressure build-up and gas evolution from the polymer are conceivable. Since many cracks appeared to be initiated from the central areas between the fibers, according to higher magnification SEM micrographs (Fig. 8), pressure applied during consolidation was the most probable cause. As the filler content in the matrix precursor increased, the intervals between the fibers became larger, and the strength of its pyrolyzed product might have weakened. Consequently, the mechanical resistance of the consolidated body against the applied load would decline, and the cracks would be initiated. This kind of crack would also contribute to the decline of the relative density going from 57 to 67% filler. In Fig. 7(b), a fairly well-densified microstructure avoiding both types of defects was observed.

For closer inspection of the polymeric slurry-derived matrix and fiber/matrix interface, TEM micrographs taken after multiple PIP processing are exhibited in Fig. 9. Micrographs (A), (B) and (C) represent the microstructures of the composites obtained for filler contents of 25, 57 and 67%, respectively. Micrograph (D) is a microstructure obtained by multiple densification with PCS. In all composites, it was found that the polymer-pyrolyzed product adhered well to the Hi-Nicalon™ fibers and that the SiC particles were dispersed homogeneously. These results are due to the good permeability, wettability and dispersibility of PVS and of the

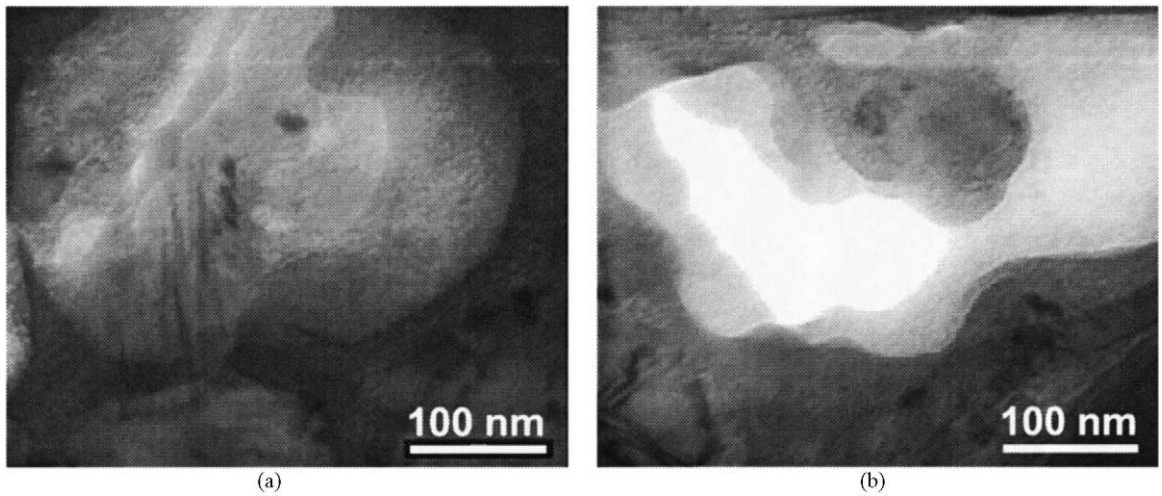

Fig. 10. TEM micrographs of a composite consolidated with a slurry of 57% filler content and multiply densified using PVS, showing scale-like structures (a) filled and (b) not filled with the polymer-pyrolyzed product.

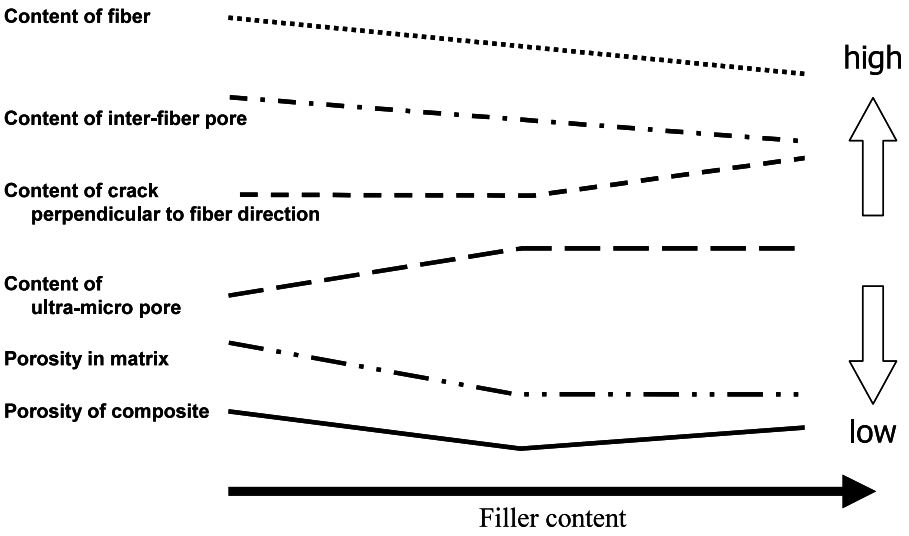

Fig. 11. Summary of the effects of filler content on microstructure.

PCS solution. There could be seen many speckles distributed uniformly. These morphological features are different from those obtained by CVI [41,42]. The latter were considered to be related to the pyrolytic behavior of the preceramic polymer, which was accompanied by gas evolution and volumetric change [43].

The effect of polymer used in multiple PIP processing on the ultramicrostructure can be recognized by comparing (B) and (D) in Fig. 9. Many spots of various diameters up to 500 nm are distributed in (B). Most of them were filled with pyrolyzed product, as shown in Fig. 10(a). It is considered that those structures were originally pores after consolidation and were filled by subsequent PIP processing. The scale-like morphology might be attributed to the pyrolytic behavior of PVS. On the other hand, spots of constant diameter ($\approx$ 300 nm) were distributed in (D). Based on their distinct outlines, these appear to be pores that remained due to insufficient permeability of the PCS solution. However, the number of these pores is much fewer than that of the scale-like structures shown in (B). This might be due to the superior volumetric yield of PCS. The differences in the ultramicrostructure between (B) and (D) were consistent with those in the densification behavior shown (Fig. 5). It can again be recognized that the original PVS is superior to the PCS solution in permeability, but inferior in volumetric yield.

Differences in the ultramicrostructure depending on the SiC particle content appeared in the sizes of the speckles, as shown in Fig. 9(A)–(C). The diameters in (A) were 200 nm at most and increased up to 500 nm in (B). No noticeable change in diameter was seen in going from (B) to (C). It was apparent that the sizes of the ultramicropores increased as the SiC particle content rose to 57%. As described above, many of these speckles were already filled with polymer-pyrolyzed product, but some of the large ones remained as pores, as represented in Fig. 10(b). These kinds of pores were considered to be formed due to drastic shrinkage of the precursor between the SiC particles. If evolved gas were efficiently emitted, polymer-pyrolyzed product in the slurry would rapidly agglomerate to make a tight matrix with a small number of pores. On the other hand, if efficient gas emission were hindered by the presence of numerous

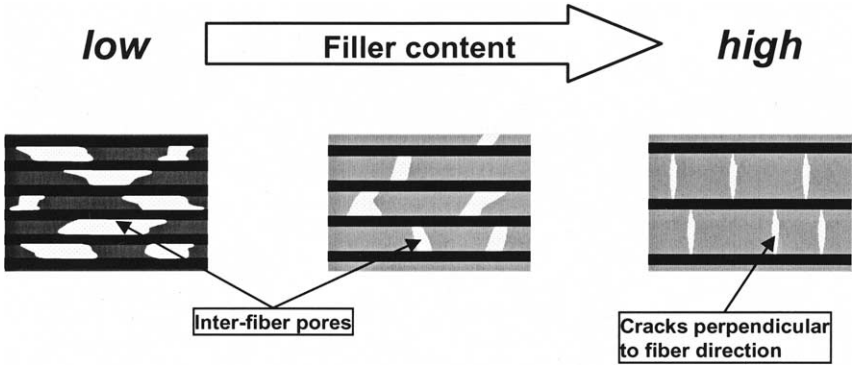

Fig. 12. Schematic illustration of the microstructures consolidated with various filler content slurries, representing the effect of filler content on the fiber volume fraction and matrix microstructure.

Table 2
Mechanical properties of the composites

ID	Filler content (%)	Polymer for multiple PIP	V_f (%)	Porosity (%)	σ_{uf} (MPa)	E_f (GPa)	WOF (kJ m^{-2})
1	25	PVS	55	18.7	334	136	1.7
2	57	PVS	38	18.9	602	135	5.1
3	67	PVS	31	19.8	575	119	4.3
4	57	PCS	38	20.1	593	108	5.0

particles, gas would remain in the matrix, resulting in the formation of pores.

Based on the above experimental data, the effect of the SiC particle content in the polymeric slurry on the microstructure of the consolidated bodies is summarized in Fig. 11. The changes in the microstructure are schematically illustrated in Fig. 12. When a fibrous preform impregnated with low filler-content slurry was consolidated, many pores were generated in inter-fiber areas due to large shrinkage of the slurry. With increasing filler content, the number of these pores was reduced owing to the improvement of effective volumetric yield of the matrix precursor. At the same time, the fiber volume fraction decreased continuously due to the decline of the fluidity of the slurry. When the filler content was increased further, cracks were initiated perpendicular to the fiber direction, mainly due to the pressure applied during consolidation. Ultramicropores were distributed in the matrices of all of the composites due to volumetric shrinkage of the polymer precursor. These pores were enlarged due to the interaction with SiC particles, as the filler content was increased to a certain degree. The porosity of the consolidated bodies was determined by the relationship between the fiber volume fraction and the porosity of the matrix, and it was minimized at the filler content that avoided the formation of both inter-fiber pores and cracks perpendicular to the fiber direction.

Table 2 shows the mechanical properties of the composites. Flexural strengths and WOFs were closely dependent on the porosity after consolidation. As a remarkable accomplishment, the composite based on 57% filler reached 600 MPa of flexural strength and 5 kJ m^{-2} of WOF. The composite based on 25% filler showed the lowest performance, although it could be densified most after multiple PIP processing. This should be due to inter-fiber pores still remaining after multiple PIP processing. Thus, inter-fiber densification seemed to be one of the main negative factors in determining mechanical performance. The composite for 67% filler was also inferior to that for 57%, especially in the tangent modulus of elasticity E_f, which might be attributed to the lowest fiber volume fraction and cracks perpendicular to the fiber direction. These results suggest that the consolidation conditions are very important for making high performance composites. Comparing E_f values for the composite multiply densified with PVS with that for the composite densified with PCS, the latter proved to be lower, which might be related to matrix microstructural features such as the distribution of ultramicropores. This issue of microstructure holds strong interest for future work to improve the mechanical properties of polymer-derived composites.

4. Conclusions

To improve the performance of SiC/SiC composites, a PIP process was developed with systematic control of the SiC particle loading. PVS showed excellent permeability and wettability with SiC particles and Hi-Nicalon™ fibers. A remarkable reduction of porosity was accomplished for optimized filler content. This was aided by efficient reduction of the numbers of pores and cracks in the consolidated body. The nanostructure of the matrix and fiber/matrix interfaces had a close relationship with the characteristics of the polymer and filler content. The reduction of flaws in the consolidated body resulted in a remarkable improvement in the mechanical properties. The feasibility of high-strength SiC/SiC composite production with polymer precursors has thus been amply demonstrated.

Acknowledgements

This work was performed as a part of an 'R&D of Composite Materials for Advanced Energy Systems' research project, supported by Core Research for Evolutional Science and Technology (CREST). The authors are grateful to Dr M. Itoh (Mitsui Chemicals, Inc., Japan) for providing a sample of PVS.

References

[1] A. Kohyama, Y. Katoh, T. Hinoki, W. Zhang, M. Kotani, Proceedings of Eighth European Conference on Composite Materials, Naples, Italy, June 3–6, 1998, vol. 4, Woodhead Publishing, Cambridge, 1998, p. 15.
[2] L.L. Snead, R. Jones, A. Kohyama, P. Fenici, J. Nucl. Mater. 26–36 (1996) 233.
[3] D. Brewer, Mater. Sci. Eng. A261 (1999) 284.

[4] F.I. Hurwitz, J.Z. Gyekenyesi, P.J. Conroy, Ceram. Eng. Sci. Proc. 10 (7) (1989) 750.
[5] K. Nakano, A. Kamiya, H. Okuda, in: R.B. Bhagat, A.H. Clauer, P. Kumar, A.M. Ritter (Eds.), Metal and Ceramic Matrix Composites: Processing, Modeling and Mechanical Behavior, The Minerals, Metals and Materials Society, 1990, p. 185.
[6] H. Yoshida, N. Miyata, M. Sagawa, S. Ishikawa, K. Naito, N. Enomoto, C. Yamagishi, J. Ceram. Soc. Jpn 100 (4) (1992) 454.
[7] D. Shin, H. Tanaka, J. Am. Ceram. Soc. 77 (1) (1994) 97.
[8] T. Tanaka, N. Tamari, I. Kondoh, M. Iwasa, J. Ceram. Soc. Jpn 103 (1) (1995) 1.
[9] M. Takeda, Y. Imai, H. Ichikawa, Y. Kagawa, H. Iba, H. Kakisawa, Ceram. Eng. Sci. Proc. 18 (1997) 779.
[10] K. Sato, A. Tezuka, O. Funayama, T. Isoda, Y. Terada, S. Kato, M. Iwata, Compos. Sci. Technol. 59 (1999) 853.
[11] R. Jones, A. Szweda, D. Petrak, Composites: Part A 30 (1999) 569.
[12] J.A. Cornie, Y. Ching, D.R. Uhlmann, A. Mortensen, J.M. Collins, Am. Ceram. Soc. Bull. 65 (1986) 293.
[13] E. Fitzer, R. Gadow, Am. Ceram. Soc. Bull. 65 (1986) 326.
[14] P.J. Lamicq, G.A. Bernhart, M.M. Dauchier, J.G. Mace, Am. Ceram. Soc. Bull. 65 (2) (1986) 336.
[15] F. Sirieix, P. Goursat, A. Lecomte, A. Dauger, Compos. Sci. Technol. 37 (1990) 7.
[16] J.A. Lewis, M.J. Cima, W.E. Rhine, J. Am. Ceram. Soc. 77 (1994) 1839.
[17] G.D. Soraru, in: J. Bill, F. Wakai, F. Aldinger (Eds.), Precursor-Derived Ceramics, Wiley–VCH, Netherlands, 1999, p. 93.
[18] P. Colombo, T.E. Paulson, C.G. Pantano, J. Am. Ceram. Soc. 80 (9) (1997) 2333.
[19] S. Yajima, Y. Hasegawa, K. Okamura, T. Matsuzawa, Nature 273 (5663) (1978) 525.
[20] R.E. Tressler, Composites: Part A 30 (1999) 429.
[21] T. Ishikawa, Y. Kohtoku, K. Kumagawa, T. Yamamura, T. Nagasawa, Nature 391 (1998) 773.
[22] G. Passing, R. Riedel, H. Schonfelder, R.J. Brook, in: G. Ziegler, H. Hausner (Eds.), Euro-Ceramics II, vol. 2, Deutsche Keramische Gesellschoft, Koln, 1992, p. 601.
[23] R. Riedel, G. Passing, H. Schonfelder, R.J. Brook, Nature 355 (1992) 714.
[24] J. Jamet, J.R. Spann, R.W. Rice, D. Lewis, W.S. Coblenz, Ceram. Eng. Sci. Proc. 5 (7) (1984) 677.
[25] D. Suttor, T. Erny, P. Grail, H. Goedeke, T. Hung, Ceramic science and processing technology, in: H. Hausner, S. Hirano, G.L. Messing (Eds.), Ceramic Transaction, vol. 51, American Ceramic Society, Westerville, OH, 1995, p. 211.
[26] Y. Hasegawa, K. Okamura, J. Mater. Sci. 18 (1983) 3633.
[27] K. Okamura, Composite 18 (2) (1987) 107.
[28] G.D. Soraru, F. Babonneau, J.D. Mackenzie, J. Mater. Sci. 25 (1990) 3886.
[29] M. Itoh, K. Iwata, M. Kobayashi, R. Takeuchi, T. Kabeya, Macromolecules 31 (1998) 5609.
[30] B. Boury, R.J.P. Corriu, W.E. Douglas, Chem. Mater. 3 (1991) 487.
[31] W.R. Schmidt, L.V. Interrante, R.H. Doremus, T.K. Trout, P.S. Marchetti, G.E. Maciel, Chem. Mater. 3 (1991) 257.
[32] R.J.P. Corriu, D. Leclercq, P.H. Mutin, J.M. Planeix, A. Vioux, Organometallics 12 (1993) 454.
[33] G. Chollon, R. Pailler, R. Naslain, F. Laanani, M. Monthioux, P. Olry, J. Mater. Sci. 32 (1997) 327.
[34] G. Chollon, M. Czerniak, R. Pailler, X. Bourrat, R. Naslain, J.P. Pillot, R. Cannet, J. Mater. Sci. 32 (1997) 893.
[35] M. Kotani, A. Kohyama, K. Okamura, T. Inoue, Ceram. Eng. Sci. Proc. 20 (4) (1999) 309.
[36] Y. Katoh, A. Kohyama, T. Hinoki, W. Yang, W. Zhang, Ceram. Eng. Sci. Proc. 21 (3) (2000) 399.
[37] ASTM Designation C1341-97, 1998 Annual Book of ASTM Standards, 15.01, 1998.
[38] V. Kostopoulos, L. Vellios, Y.Z. Pappas, J. Mater. Sci. 32 (1997) 215.
[39] T. Ishikawa, M. Shibuya, T. Hirokawa, Proceedings of Japan–Europe Symposium on Composite Materials, Japan Industrial Technology Association, 1993, p. 185.
[40] N. Miriyala, P.K. Liaw, C.J. McHargue, L.L. Snead, J. Nucl. Mater. 1 (1998) 253.
[41] T. Hinoki, W. Zhang, Y. Katoh, A. Kohyama, H. Tsunakawa, Proceedings of Eighth European Conference on Composite Materials, Naples, Italy, June 3–6, 1998, vol. 4, Woodhead Publishing, Cambridge, 1998, p. 209.
[42] Y. Xu, L. Cheng, L. Zhang, W. Zhou, J. Mater. Sci. 34 (1999) 551.
[43] R. Chain, A.H. Heuer, R.T. Chen, J. Am. Ceram. Soc. 71 (11) (1988) 960.